

## Full Length Article

# Pilot-scale optimization of a physical–chemical biogas upgrading system based on a high alkalinity absorbent at ambient pressure and temperature

Edwin G. Hoyos <sup>a,b</sup> , Saeed Rasekhi <sup>a</sup> , Rogelio Mazaeda <sup>a,c</sup> , Raúl Muñoz <sup>a,b,\*</sup>

<sup>a</sup> Institute of Sustainable Processes, University of Valladolid, Dr. Mergelina, s/n, 47011 Valladolid, Spain

<sup>b</sup> Department of Chemical and Environmental Engineering, University of Valladolid, Dr. Mergelina, s/n, 47011 Valladolid, Spain

<sup>c</sup> Department of Systems Engineering and Automation, University of Valladolid, Dr. Mergelina, s/n, 47011 Valladolid, Spain

## ARTICLE INFO

## ABSTRACT

## Keywords:

Biogas chemical absorption  
Biomethane  
Carbon-coated iron nanoparticles  
EDTA-Fe/carbonate solution  
EN 16723

The optimization of an innovative process consisting of chemical absorption–desorption at ambient pressure and temperature with EDTA-Fe/carbonate solutions devoted to biogas upgrading was conducted. The influence of parameters such as the initial pH (9–10), inorganic carbon concentration (IC) (4000–8000 mg/L), biogas flowrate (BF) (30–90 L/d), air flowrate (AF) (300–1500 L/d), L/G ratio (0.7–3) and EDTA-Fe concentration (Fe) (0–30 mM) on biomethane composition was evaluated. In addition, the effect of carbon-coated iron nanoparticles on CO<sub>2</sub> absorption performance was investigated. The L/G ratio governed the O<sub>2</sub> concentration in the biomethane. Interestingly, the addition of EDTA-Fe was not necessary for the complete removal of H<sub>2</sub>S from the biogas. BF, AF and IC exerted a significant influence on the biomethane CO<sub>2</sub> concentration (BF > AF > IC), while the initial pH induced no effect. On the other hand, the supplementation of iron nanoparticles did not significantly influence on the CO<sub>2</sub> absorption performance. The optimal conditions in a 7 L absorption-7 L desorption system were: BF = 90 L/d, AF = 1500 L/d, L/G = 0.7, IC = 8000 mg C/L, initial pH = 9.5 and Fe = 0 mM. Under these operational conditions, the biomethane obtained was free of H<sub>2</sub>S and average concentrations of CO<sub>2</sub>, O<sub>2</sub>, N<sub>2</sub> and CH<sub>4</sub> of 1.7 ± 0.1 %, 0.7 ± 0.1 %, 2.7 ± 0.5 % and 94.9 ± 0.6 %, respectively, were recorded for 3 weeks of continuous operation. This biomethane complied with the European standard EN 16273 on the biomethane use for injection into natural gas networks.

## 1. Introduction

Today, conventional physical–chemical technologies are still the most widely used for cleaning and upgrading biogas on an industrial scale [1]. However, these techniques require high inputs of energy and chemicals, and do not support the simultaneous removal of CO<sub>2</sub> and H<sub>2</sub>S from biogas in a single step, which entails high capital and operational costs [2,3]. In this context, research and development of more cost-effective and environmentally sustainable technologies should be promoted to address global challenges of energy security and global warming [4].

Emerging biogas upgrading technologies, such as inorganic solvent scrubbing, in-situ methane enrichment or biological methods, exhibit lower capital and operating costs, high efficiency, and lower environmental impacts compared to conventional technologies, although they are still in the development stage [5]. In this context, the absorption–desorption of CO<sub>2</sub> combined with H<sub>2</sub>S oxidation based on aqueous

carbonate and EDTA-Fe solutions represent a cost-effective and sustainable technology for the simultaneous removal of CO<sub>2</sub> and H<sub>2</sub>S from biogas [3]. In this process, the CO<sub>2</sub> from biogas is efficiently captured in the absorption column as a result of the high alkalinity and pH of the scrubbing solution and the biogas microbubbles flowing upwards counter-currently to the aqueous solution, thus favouring the CO<sub>2</sub> gas–liquid mass transfer. The CO<sub>2</sub>-laden solvent is regenerated in the stripping column via air-aided CO<sub>2</sub> desorption and the regenerated solvent is recirculated to the scrubbing column. On the other hand, the presence of EDTA-Fe(III) supports an efficient H<sub>2</sub>S removal via oxidation to sulphur with the concomitant reduction of Fe<sup>3+</sup> to Fe<sup>2+</sup>. In addition, the resulting EDTA-Fe(II) solution can be regenerated in the desorption/regeneration column via oxidation of Fe<sup>2+</sup> to Fe<sup>3+</sup> using the same air used for CO<sub>2</sub> stripping [6]. Therefore, this process represents a promising and sustainable technology for biogas cleaning/upgrading based on the absence of a continuous supply of chemicals/materials, which allows the efficient and simultaneous removal of H<sub>2</sub>S and CO<sub>2</sub> from

\* Corresponding author at: Institute of Sustainable Processes, University of Valladolid, Dr. Mergelina, s/n, 47011 Valladolid, Spain.

E-mail address: [raul.munoz.torre@uva.es](mailto:raul.munoz.torre@uva.es) (R. Muñoz).

biogas under ambient pressure and temperature conditions. However, this technology is still in its early stages of development and needs further research to pave the way toward its industrial implementation. In this context, Marín et al. (2020) [3] validated this technology at lab scale in an absorption–desorption experimental set-up composed of 1.8 L bubble columns constructed with stainless steel 2  $\mu\text{m}$  diffusers. Unfortunately, this type of biogas diffusers entail a rapid clogging by elemental sulphur and prohibitive pressure drops, which limits the potential scale-up of the technology.

On the other hand, the use of solid nanoparticles dispersed in a liquid phase has been widely investigated due to its great potential to boost gas–liquid mass transfer [7]. In this regard, Lee et al. (2015) [8] reported an enhancement in the absorption and regeneration of  $\text{CO}_2$  in deionized water by 23.5 % and 11.8 %, respectively, using  $\text{SiO}_2$  nanoparticles. Similarly, Jeon et al. (2017) [9] improved the volumetric mass transfer coefficient ( $k_{\text{LA}}$ ) in a  $\text{CO}_2/\text{H}_2\text{O}$  system by 31 and 145 % via addition of silica ( $\text{SiO}_2$ ) and methyl-functionalized silica ( $\text{SiO}_2\text{-CH}_3$ ) nanoparticles, respectively. On the other hand, the addition of carbon coated iron based nanoparticles (CCINs) to the algal-bacterial cultivation broth of photobioreactors has proven to be an effective strategy to increase  $\text{CO}_2$  removal efficiency during photosynthetic biogas upgrading, although the mechanisms underlying this enhancement remain unclear [10,11]. Finally, the effect of CCINs on the performance of absorption–desorption processes devoted to biogas upgrading has not yet been tested.

One of the main limitations of conventional biogas upgrading technologies is the requirement of two separate processes for the removal of  $\text{H}_2\text{S}$  and  $\text{CO}_2$ . Another important limitation is the need for high pressure and temperatures, which makes their investment and operating costs high. This novel technology is capable of simultaneously removing  $\text{H}_2\text{S}$  and  $\text{CO}_2$  from biogas under ambient pressures and temperatures. In this sense, this research represents the first study on the optimization of process variables of an absorption–desorption biogas upgrading system based on carbonate and EDTA-Fe solutions at pilot scale with membrane diffusers (to overcome the limitation of rapid clogging by elemental sulphur and excessive pressure drops encountered in the stainless steel 2  $\mu\text{m}$  diffusers previously reported in literature) and under conditions of ambient temperature and pressure, with the main goal of achieving a biomethane complying with European regulations ( $\text{CO}_2 \leq 2\%$ ,  $\text{O}_2 \leq 1\%$ ,  $\text{CH}_4 \geq 90\%$  and negligible concentrations of  $\text{H}_2\text{S}$ ) for its injection into natural gas grids. In addition, this work evaluated for the first time the influence of CCINs on the performance of absorption–desorption biogas upgrading. Finally, this work discussed and demonstrated, for the

first time, the  $\text{H}_2\text{S}$  removal mechanisms in this process when EDTA-Fe was not supplemented.

## 2. Materials and methods

### 2.1. Biogas, solvent and nanoparticles

Synthetic biogas with a composition of 65 %  $\text{CH}_4$ , 34.5 %  $\text{CO}_2$ , 0.5 %  $\text{H}_2\text{S}$ , supplied by Carburos Metálicos (Spain), was used to simulate raw biogas. Iron (III) monosodium ethylenediaminetetraacetic (Sigma-Aldrich, USA),  $\text{Na}_2\text{CO}_3$  and  $\text{NaHCO}_3$  (Solvay Chemicals International SA, Spain) were used to prepare the carbonate/EDTA-Fe absorbent. The characterization of the two types of carbon coated iron-based nanoparticles herein used (chemical composition, porosity, surface area, size, and SEM image) can be found in [Supplementary material](#).

### 2.2. Experimental set-up

The chemical biogas scrubbing system consisted of an absorption column and a regeneration column with similar characteristics ( $D = 6.7\text{ cm}$ ;  $H = 2.7\text{ m}$ ; working volume = 7.2 L) ([Fig. 1](#)). The carbonate/EDTA-Fe scrubbing solution was pumped from the bottom of the absorption column to the top of the stripping column by a peristaltic pump (Dinko Instruments, Spain). The regenerated absorbent solution was returned to the scrubbing column by gravity after previously passing through a conical degassing and elemental sulphur accumulation chamber of 2.8 L ( $D = 14.5\text{ cm}$ ;  $H = 21.5\text{ cm}$ ). Biogas was sparged in fine bubbles at the bottom of the absorption column via a membrane diffuser of 0.6  $\mu\text{m}$  pore size under counter-current flow operation. Likewise, air was sparged at the bottom of the regeneration column through a membrane diffuser of 0.6  $\mu\text{m}$  pore size under counter-current flow operation. The biogas and air flow rates were controlled using a mass flow controller (Aalborg, USA) and a rotameter (Aalborg, USA), respectively. The experimental set-up was placed at the Institute of Sustainable Processes of Valladolid University (Spain).

### 2.3. Operating conditions and sampling monitoring

All experiments were carried out under a controlled temperature of 20 °C in duplicate. Six operational parameters were evaluated to optimize the process of upgrading biogas to biomethane and comply with biomethane regulations for injection into natural gas grids or use as

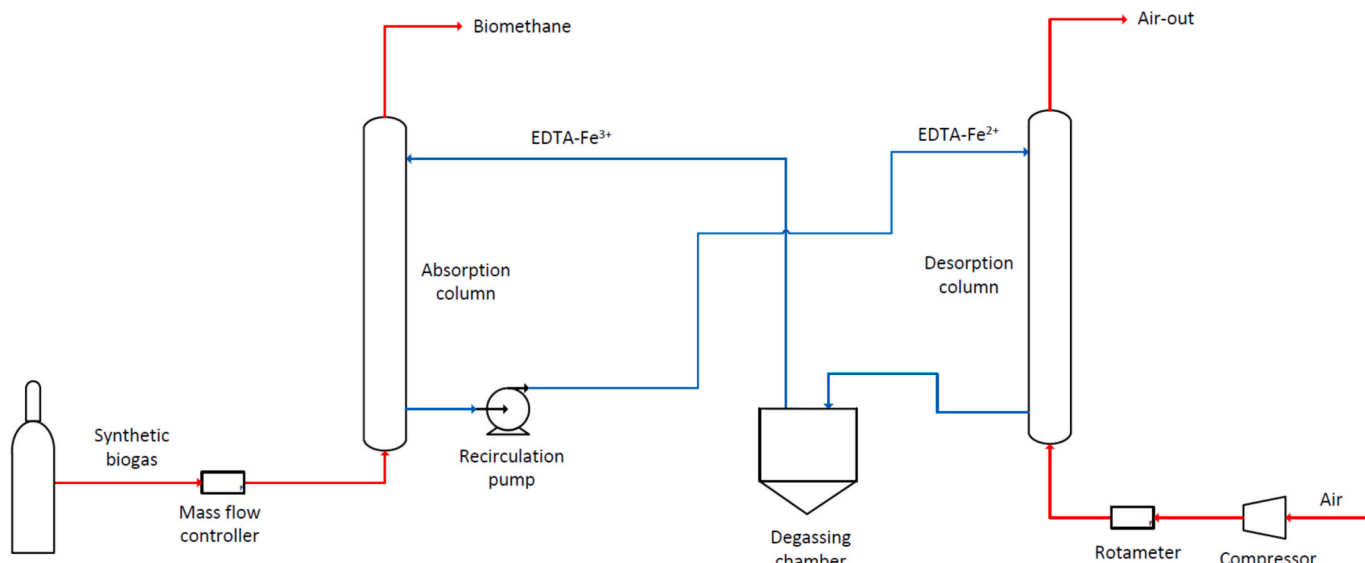


**Fig. 1.** Experimental set-up of the absorption–desorption process for the simultaneous removal of  $\text{CO}_2$  and  $\text{H}_2\text{S}$  from biogas. Red lines: gas streams; Blue lines: liquid streams. (For interpretation of the references to colour in this figure legend, the reader is referred to the web version of this article.)

automotive fuel ( $\text{CO}_2 \leq 2\%$ ,  $\text{O}_2 \leq 1\%$ ,  $\text{CH}_4 \geq 90\%$  and minor traces of  $\text{H}_2\text{S}$ ) [12,13]: pH, inorganic carbon concentration (IC), air flow rate (AF), biogas flow rate (BF), EDTA-Fe molarity (Fe) and recirculating liquid/biogas flow rate ratio (L/G). The basis for the selection of these parameters and their ranges was the study conducted by Marín et al [3]. According to the literature, Fe is an crucial parameter influencing the removal of  $\text{H}_2\text{S}$ , while L/G is the factor governing the stripping of  $\text{O}_2$  and  $\text{N}_2$  from the scrubbing solution to the biomethane [3]. Therefore, preliminary experiments were performed to set a value for these two parameters in order to achieve a complete removal of  $\text{H}_2\text{S}$  and a biomethane  $\text{O}_2$  concentration lower than 1 %. This variable allocation allowed reducing the number of experiments. The optimization of the remaining operational parameters, with the aim of reducing the biomethane  $\text{CO}_2$  concentration below 2 %, was carried out through a Taguchi experimental design. Three levels were selected for the study parameters (Table 1), which resulted in a L9 Taguchi orthogonal array design ( $3^4$ ) [14]. The design of the experiments using the Taguchi method significantly reduced the experimental load without losing relevant information for future decision making based on the results of the experiments. In this particular case, the Taguchi method reduced the number of experiments from  $3^4 = 81$  (required by a full factorial design) to 9 (Table 1). The optimal experimental conditions to meet the biomethane standard EN 16723 under the maximum biogas flow rate of 90  $\text{L d}^{-1}$  were then investigated in experiments conducted in duplicate. No addition of EDTA-Fe was tested under the optimal experiment conditions in order to determine the inherent capacity of the process to remove  $\text{H}_2\text{S}$  without the contribution of EDTA-Fe. The effect of the addition of two types of carbon coated iron nanoparticles on  $\text{CO}_2$  absorption at concentrations of 300 and 3000  $\text{mg L}^{-1}$  was investigated in tests performed in duplicate under initial pH = 9, BF = 90 L/d, IC = 6000 mg/L, AF = 900 L/d, L/G = 0.7, Fe = 5 mM, which corresponded to conditions not fulfilling the biomethane standard in terms of  $\text{CO}_2$  content. Finally, two continuous experiments were conducted for 21 days under optimal conditions (one with EDTA-Fe addition and one without) to validate the process stability under continuous operation.

Gas composition was monitored (using a 100  $\mu\text{L}$  of gas-tight syringe) every two hours for the experiments carried out to set the Fe and L/G values. The duration of these experiments (6–21 h) was sufficient to ensure the stability of the concentration of  $\text{O}_2$  and  $\text{N}_2$  in the biomethane. For the rest of the experiments, gas composition, pH and IC concentration of the scrubbing solution (using 10 mL of sample) were monitored daily until steady-state conditions were achieved (1–10 d). The continuous biogas upgrading experiments included also the monitoring of the concentration of dissolved  $\text{H}_2\text{S}$ , thiosulphate and sulphate in the solvent in order to determine the fate of the  $\text{H}_2\text{S}$  removed from the biogas.

#### 2.4. Analytical methods

The pH was measured using a pH-meter BASIC 20+ (Crison Instruments, Spain). The IC concentration was determined using a Shimadzu TOC-L analyser (Japan). The composition of biogas and biomethane ( $\text{CO}_2$ ,  $\text{H}_2\text{S}$ ,  $\text{O}_2$ ,  $\text{N}_2$  and  $\text{CH}_4$ ) was analysed using a gas

chromatograph with a thermal conductivity detector (Agilent 8860 GC System, USA) according to [15]. The concentration of dissolved  $\text{H}_2\text{S}$  was determined using a sulphide test kit (Supelco) in a Shimadzu UV-2550 spectrophotometer (Japan) at 665 nm. Finally, the sulphate and thiosulphate concentrations were measured by HPLC-IC (Waters 432, ion conductivity detector, USA).

#### 2.5. Statistical treatment

The results under steady state conditions (minimum two measurements under steady-state) are presented as the mean value with its respective standard deviation. Taguchi method was used for experimental design. The Spearman correlation coefficient was determined to assess the strength and direction of the relationship between the manipulated variables and the variable to be optimized.

### 3. Results and discussion

#### 3.1. Determination of Fe content and L/G ratio for $\text{CO}_2$ absorption optimization

Tables 2 and 3 show the conditions and results of the experiments carried out for the determination of the optimal values of Fe and L/G set for further optimization of  $\text{CO}_2$  removal from biogas. The  $\text{O}_2$  concentration in the biomethane accounted for 3, 2 and 1 % v/v when the L/G ratio was 3, 2 and 1, respectively, while the  $\text{N}_2$  concentration averaged ~6, ~5 and 3 % v/v, respectively (Table 3).  $\text{O}_2$  concentrations of 0.8–0.9 % and  $\text{N}_2$  concentrations of 2–3 % v/v were recorded at a L/G ratio of 0.7. These results were in line with the research carried out by Toledo-cervantes et al. (2016) [16] and Posadas et al. (2017) [17], who reported that the higher the L/G ratio, the higher the concentration of  $\text{O}_2$  and  $\text{N}_2$  in the biomethane, with biomethane  $\text{O}_2$  and  $\text{N}_2$  concentrations decreasing below 1 % and 2–3 % v/v, respectively, at only L/G ratios <1.

On the other hand, a 5 mM EDTA-Fe concentration supported a complete removal of  $\text{H}_2\text{S}$ , even at the lowest L/G ratios of 0.7 and a maximum biogas flow rate of 90  $\text{L d}^{-1}$ . In this context, Schiavon et al. (2017) [6] achieved a  $\text{H}_2\text{S}$  removal efficiency of 97.8 % in a 840 L pilot plant operated at an EDTA-Fe concentration of 190 mM, a L/G of 1.19 and a biogas flow rate of 600  $\text{m}^3 \text{d}^{-1}$  with 0.5 % v/v of  $\text{H}_2\text{S}$ , and a  $\text{H}_2\text{S}$  removal efficiency of 91.4 % in a 0.5 L lab-scale system operated at a EDTA-Fe concentration of 200 mM, a L/G of 1.0 and a biogas flow rate of 340  $\text{mL min}^{-1}$  containing 2.2 % v/v of  $\text{H}_2\text{S}$ . Similarly, Frare et al. (2010) [18] achieved a complete elimination of  $\text{H}_2\text{S}$  operating at a L/G ratio of 0.46, with an EDTA-Fe concentration of 400 mM at a biogas flow rate of 265  $\text{mL min}^{-1}$  (2.2 % v/v of  $\text{H}_2\text{S}$ ) in a 1 L lab-scale system. Marín et al. (2020) [3] achieved a  $\text{H}_2\text{S}$  removal efficiency of 96.8 % operating at a L/G of 3 with an EDTA-Fe concentration of 30 mM and a biogas flow rate of 10  $\text{mL min}^{-1}$  (0.5 % v/v of  $\text{H}_2\text{S}$ ) in a 4 L lab-scale plant, and a complete  $\text{H}_2\text{S}$  removal when the EDTA-Fe concentration was increased up to 50 mM. Overall, the EDTA-Fe concentration of 5 mM herein used was much lower than those used in the literature for a complete removal of  $\text{H}_2\text{S}$  under similar L/G ratios. For the further optimization of  $\text{CO}_2$  removal, a L/G = 0.7 and [Fe] concentration of 5 mM were set in the pilot plant.

**Table 1**

Taguchi experimental design L9 ( $3^4$ ) for the optimization of  $\text{CO}_2$  removal from biogas (all experiments were conducted at [Fe] = 5 mM and L/G = 0.7).

Experiment	pH	IC (mg/L)	BF (L/d)	AF (L/d)
1	9.0	4000	60	300
2	9.5	6000	60	600
3	10.0	8000	60	900
4	9.0	6000	90	900
5	9.5	8000	90	300
6	10.0	4000	90	600
7	9.0	8000	30	600
8	9.5	4000	30	900
9	10.0	6000	30	300

**Table 2**

Experimental conditions for the determination of the optimal Fe content and L/G ratio for further optimization of  $\text{CO}_2$  removal from biogas.

Experiments	Initial pH	IC (mg $\text{L}^{-1}$ )	BF (L $\text{d}^{-1}$ )	AF (L $\text{d}^{-1}$ )	Fe (mM)	L/G
1	9	6000	60	900	30	3.0
2	9	4000	60	600	10	2.0
3	9	8000	90	600	30	1.0
4	10	2000	90	900	5	0.7

**Table 3**

Steady state composition of biomethane during the optimization of Fe content and L/G for further optimization of CO<sub>2</sub> removal from biogas. Experiments performed in duplicate (a y b).

	Duration (h)	Biomethane (% v/v)				
		CO <sub>2</sub>	H <sub>2</sub> S	O <sub>2</sub>	N <sub>2</sub>	CH <sub>4</sub>
1a	9	3.6	N.D.	2.6 ± 0.1	5.9 ± 0.5	87.5
		4.0	N.D.	2.9 ± 0.1	6.6 ± 0.4	87.0
2a	10	3.7	N.D.	1.8 ± 0.2	4.5 ± 0.5	90.8
		3.5	N.D.	1.9	5.0	89.6
3a	6	6.1	N.D.	1.0 ± 0.1	3.1 ± 0.2	89.6
		7.2	N.D.	1.0 ± 0.0	3.0 ± 0.0	88.6
4a	21	1.8	N.D.	0.9 ± 0.1	2.9 ± 0.1	94.2
		1.8	N.D.	0.8 ± 0.1	2.1 ± 0.1	95.2

N.D. = Not detected.

### 3.2. CO<sub>2</sub> removal optimization

**Table 4** shows the results of the composition of biomethane under steady-state conditions of the Taguchi design experiments conducted in duplicate to determine the impact of the parameters studied on CO<sub>2</sub> absorption (Experiments 1 to 9). The values of pH and IC at steady state of the experiments can be found in *Supplementary material* (Table S1). Since the concentration of CO<sub>2</sub> in biomethane did not follow a normal distribution (Shapiro-Wilk test performed with p-value = 0.02 at 95 % confidence level), a Spearman's ordinal correlation was calculated to determine the strength and direction of influence between the modified parameters (BF, AF, initial IC and initial pH) and the variable to be optimized (biomethane CO<sub>2</sub> concentration). The values of Spearman correlation coefficient accounted for 0.7, -0.5, -0.1 and 0.0 for BF, AF, IC and pH, respectively, indicating a positive influence of the biogas flow rate, a negative effect of air flow rate and IC, and a negligible impact of

**Table 4**

Results of the experiments for CO<sub>2</sub> removal optimization (all experiments were conducted at [Fe] = 5 mM and L/G = 0.7).

Experiment	Time to SS (d)	BioCH <sub>4</sub> at steady-state (% v/v)				
		CO <sub>2</sub>	H <sub>2</sub> S	O <sub>2</sub>	N <sub>2</sub>	CH <sub>4</sub>
1	2	8.6 ± 0.1	N. D.	0.7 ± 0.0	2.9 ± 0.1	87.9 ± 0.1
		0.0	N. D.	0.0	0.1	0.1
2	5	3.5 ± 0.1	N. D.	0.7 ± 0.1	2.6 ± 0.4	93.7 ± 0.6
		0.0	N. D.	0.0	0.1	0.2
3	9	3.1 ± 0.0	N. D.	0.7 ± 0.0	2.7 ± 0.1	93.5 ± 0.2
		0.0	N. D.	0.0	0.1	0.5
4	1	3.0 ± 0.1	N. D.	0.8 ± 0.1	2.9 ± 0.5	93.2 ± 0.5
		0.0	N. D.	0.0	0.1	0.5
5	3	8.4 ± 0.1	N. D.	0.8 ± 0.1	2.5 ± 0.1	88.3 ± 0.1
		0.0	N. D.	0.0	0.1	0.1
6	4	8.3 ± 0.1	N. D.	0.8 ± 0.2	2.4 ± 0.4	88.5 ± 0.6
		0.0	N. D.	0.0	0.1	0.5
7	7	1.4 ± 0.1	N. D.	0.8 ± 0.0	3.1 ± 0.1	94.7 ± 0.2
		0.0	N. D.	0.0	0.1	0.2
8	1	1.2 ± 0.0	N. D.	0.7 ± 0.1	2.7 ± 0.3	95.2 ± 0.3
		0.0	N. D.	0.0	0.1	0.3
9	10	1.8 ± 0.0	N. D.	0.7 ± 0.0	2.8 ± 0.3	94.6 ± 0.4
		0.0	N. D.	0.0	0.1	0.4
10	4	2.4 ± 0.0	N. D.	0.8 ± 0.0	2.8 ± 0.1	94.0 ± 0.1
		0.0	N. D.	0.0	0.0	0.1
11	1	2.9 ± 0.1	N. D.	0.8 ± 0.1	3.0 ± 0.3	93.2 ± 0.4
		0.0	N. D.	0.0	0.3	0.4
12	2	2.1 ± 0.1	N. D.	0.8 ± 0.1	2.8 ± 0.2	94.3 ± 0.3
		0.0	N. D.	0.0	0.2	0.3
13	1	1.7 ± 0.1	N. D.	0.7 ± 0.1	2.4 ± 0.4	95.3 ± 0.5
		0.0	N. D.	0.0	0.1	0.5

N.D. = Not detected. SS = steady-state.

the initial pH. CO<sub>2</sub> concentrations in the biomethane below 2 % v/v were only achieved at a biogas flow rate of 30 L d<sup>-1</sup>, regardless of AF and IC (Table 4, Experiments 7–9).

The optimization of the operational conditions to achieve a CO<sub>2</sub> concentration in the biomethane < 2 % v/v at a biogas flow rate of 90 L d<sup>-1</sup> (Table 4, Experiments 10–13) was performed. Based on the results of the Spearman's correlation, the air flow rate was increased up to 1200 L d<sup>-1</sup> and IC was set at 6000 (Exp. 10), 4000 (Exp. 11) and 8000 mg C L<sup>-1</sup> (Exp. 12). The best performance in terms of biomethane CO<sub>2</sub> concentration (CO<sub>2</sub> = 2.1 % v/v) was obtained with an IC concentration of 8000 mg C L<sup>-1</sup>. Therefore, the air flowrate was increased up to 1500 L d<sup>-1</sup> at an IC concentration of 8000 mg C L<sup>-1</sup> (Exp. 13). Under these conditions, a high-quality biomethane was achieved (CO<sub>2</sub> < 2 % v/v, O<sub>2</sub> < 1 % v/v, CH<sub>4</sub> > 90 % v/v and negligible concentrations of H<sub>2</sub>S), fulfilling with European regulation for the use of biomethane as a substitute for natural gas in gas networks or as a fuel for vehicles [12,13].

### 3.3. Effect of nanoparticles on CO<sub>2</sub> removal performance

The dispersion of the carbon-coated iron nanoparticles in the absorbent liquid can enhance the CO<sub>2</sub> capture performance, which might be attributed to the large surface area, high thermal conductivity, small cluster size and magnetic properties of nanoparticles [19,20]. In this context, Taheri et al. (2016) [21] evaluated the ability of SiO<sub>2</sub> and Al<sub>2</sub>O<sub>3</sub> nanoparticles in diethanolamine to remove CO<sub>2</sub> and H<sub>2</sub>S from a natural gas stream and reported that CO<sub>2</sub> absorption was improved by 33 % and 40 % using 0.05 wt% of Al<sub>2</sub>O<sub>3</sub> and SiO<sub>2</sub>, respectively. Lee et al. (2016) [22] reported a positive effect of nanoparticles on absorbent regeneration during CO<sub>2</sub> capture using Al<sub>2</sub>O<sub>3</sub> nanoparticles, which enhanced the solvent regeneration performance by up to approximately 16 % compared to that of the conventional absorbent (methanol without nanoparticles). This scientific evidence promoted the study of the influence of two types of carbon coated iron nanoparticles (CCINs) on the performance of the absorption-regeneration process for biogas upgrading. The two types of nanoparticles tested differed mainly in their iron and carbon content, which were 34.1 % Fe (w/w) and 33.6 % C (w/w) (nanoparticles A), and 25.3 % Fe (w/w) and 41.8 % C (w/w) (nanoparticles B) (see *Supplementary material*).

**Table 5** shows the results of the tests carried out to determine the influence of nanoparticles on the removal of CO<sub>2</sub> from biogas. The conditions used as a baseline in the study were: initial pH = 9, BF = 90 L/d, [Fe] = 5 mM, IC = 6000 mg C/L, AF = 900 L/d and L/G = 0.7 (Exp. 4), which supported a steady-state concentration of CO<sub>2</sub> in biomethane of 3.0 ± 0.1 % v/v. The results showed that nanoparticles at 300 and 3000 mg/L did not exert a significant enhancement effect in the CO<sub>2</sub> absorption performance. The reasons underlying this finding may be nanoparticle aggregation, interfacial effects and/or chemical equilibrium achieved. In this sense, nanoparticle aggregation can limit/impair mass transfer at high nanoparticle concentrations [23]. On the other hand, the addition of nanoparticles can typically intensify interfacial

**Table 5**

Influence of CCINs type and concentration on the steady-state biomethane composition (% v/v).

Experiment	CO <sub>2</sub>	H <sub>2</sub> S	O <sub>2</sub>	N <sub>2</sub>	CH <sub>4</sub>
Base case	3.0 ± 0.1	N. D.	0.8 ± 0.1	2.9 ± 0.5	93.2 ± 0.5
Nanoparticle A – 0.3 g/L	2.9 ± 0.0	N. D.	0.8 ± 0.0	2.7 ± 0.1	93.6 ± 0.1
	0.1	N. D.	0.1	0.5	0.5
Nanoparticle B – 0.3 g/L	2.9 ± 0.1	N. D.	0.7 ± 0.1	2.7 ± 0.3	93.7 ± 0.3
	0.1	N. D.	0.1	0.3	0.3
Nanoparticle A – 3.0 g/L	3.1 ± 0.1	N. D.	0.6 ± 0.1	2.8 ± 0.4	93.5 ± 0.5
	0.1	N. D.	0.1	0.4	0.5
Nanoparticle B – 3.0 g/L	3.1 ± 0.0	N. D.	0.6 ± 0.1	2.7 ± 0.3	93.6 ± 0.4
	0.0	N. D.	0.1	0.3	0.4

N.D. = Not detected.

mass transfer by increasing the interfacial area and/or decreasing the interfacial tension, thus improving the solute gas–liquid mass transfer [24]. In our particular case, it may be possible that CCINs had no significant effect on interfacial mass transfer. Another hypothesis to explain the limited impact of nanoparticles may be that chemical equilibrium between the biogas and liquid phase was already reached under the baseline conditions (absence of nanoparticles). Related to the latter, the determination of the volumetric coefficient of mass transfer ( $k_{L,a}$ ) (with and without nanoparticles) could indicate whether equilibrium had already been reached in the absence of nanoparticles, and in this case the nanoparticles could decrease the time required to reach equilibrium,

and therefore, the volume of the system.

### 3.4. Operation in the absence of EDTA-Fe and validation of the system in continuous operation

The complete removal of  $\text{H}_2\text{S}$  recorded under low concentrations of EDTA-Fe (compared to literature [6,18]) promoted the evaluation of process performance without the addition of EDTA-Fe. An experiment in duplicate was carried out under the optimal conditions previously identified for  $\text{CO}_2$  removal but without the addition of EDTA-Fe (BF = 90 L/d, AF = 1500 L/d, IC = 8000 mg/L, initial pH = 9.5 and L/G = 0.7).

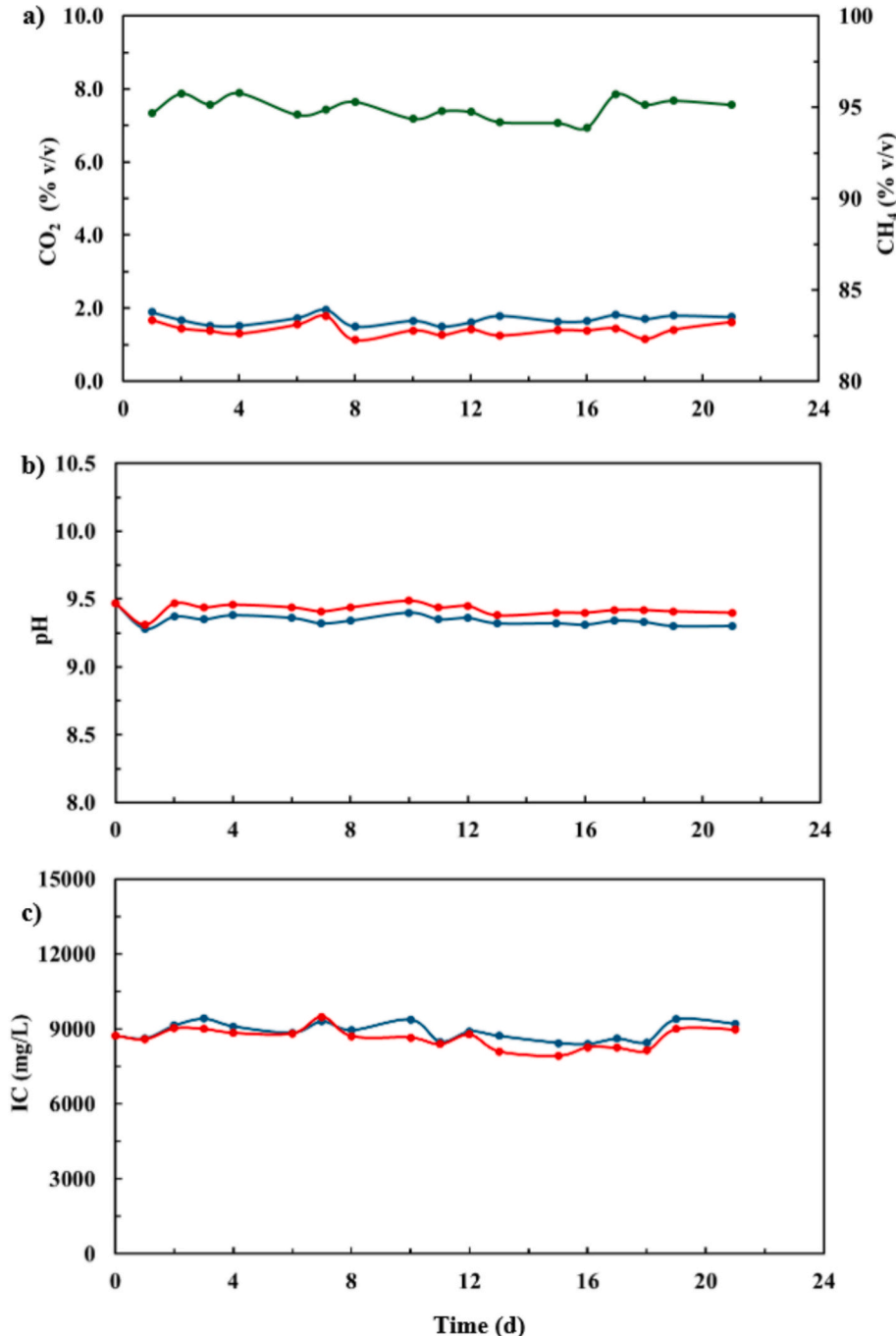


**Fig. 2.** Time course of a) biomethane  $\text{CO}_2$  concentration (blue line),  $\text{CO}_2$  concentration in the outlet air (red line) and biomethane  $\text{CH}_4$  concentration (green line); b) pH in the absorption column (blue line) and pH in the desorption column (red line); and c) IC in the absorption column (blue line) and IC in the desorption column (red line). Optimal operating conditions: BF = 90 L/d, AF = 1500 L/d, IC = 8000 mg/L, initial pH = 9.5, L/G = 0.7 and Fe = 0 Mm. (For interpretation of the references to colour in this figure legend, the reader is referred to the web version of this article.)

No  $\text{H}_2\text{S}$  was detected in the biomethane during the three days of the experiment. The steady-state concentrations of  $\text{CO}_2$ ,  $\text{O}_2$ ,  $\text{N}_2$  and  $\text{CH}_4$  in the biomethane were  $1.7 \pm 0.1\%$ ,  $0.7 \pm 0.1\%$ ,  $2.5 \pm 0.3\%$  and  $95.2 \pm 0.5\%$  v/v, respectively.

To validate the results under continuous operation, two 3-week experiments were performed under optimal conditions for  $\text{CO}_2$  removal with and without EDTA-Fe supplementation. During these experiments, the concentration of  $\text{H}_2\text{S}$ , sulphate and thiosulphate in the absorbent liquid was periodically monitored in order to understand the fate of the  $\text{H}_2\text{S}$  from the biogas.

Fig. 2 shows the results of the continuous operation of the process for 3 weeks under the above described optimal conditions in the absence of EDTA-Fe. The  $\text{CO}_2$ ,  $\text{O}_2$ ,  $\text{N}_2$  and  $\text{CH}_4$  concentrations in the biomethane averaged  $1.7 \pm 0.1\%$ ,  $0.7 \pm 0.1\%$ ,  $2.7 \pm 0.5\%$  and  $94.9 \pm 0.6\%$  v/v, respectively. The composition of the air at the outlet averaged  $1.4 \pm 0.2\%$   $\text{CO}_2$ ,  $19.9 \pm 0.2\%$   $\text{O}_2$ ,  $78.4 \pm 0.2\%$   $\text{N}_2$  and  $0.3 \pm 0.1\%$  v/v  $\text{CH}_4$ . Based on these results, a  $\text{CO}_2$  removal efficiency of 97% with a methane slip of 6% was achieved. This significant methane loss was due to the high air flow used for solvent regeneration, which likely resulted in the complete stripping of  $\text{CH}_4$  in the desorption column. An improvement

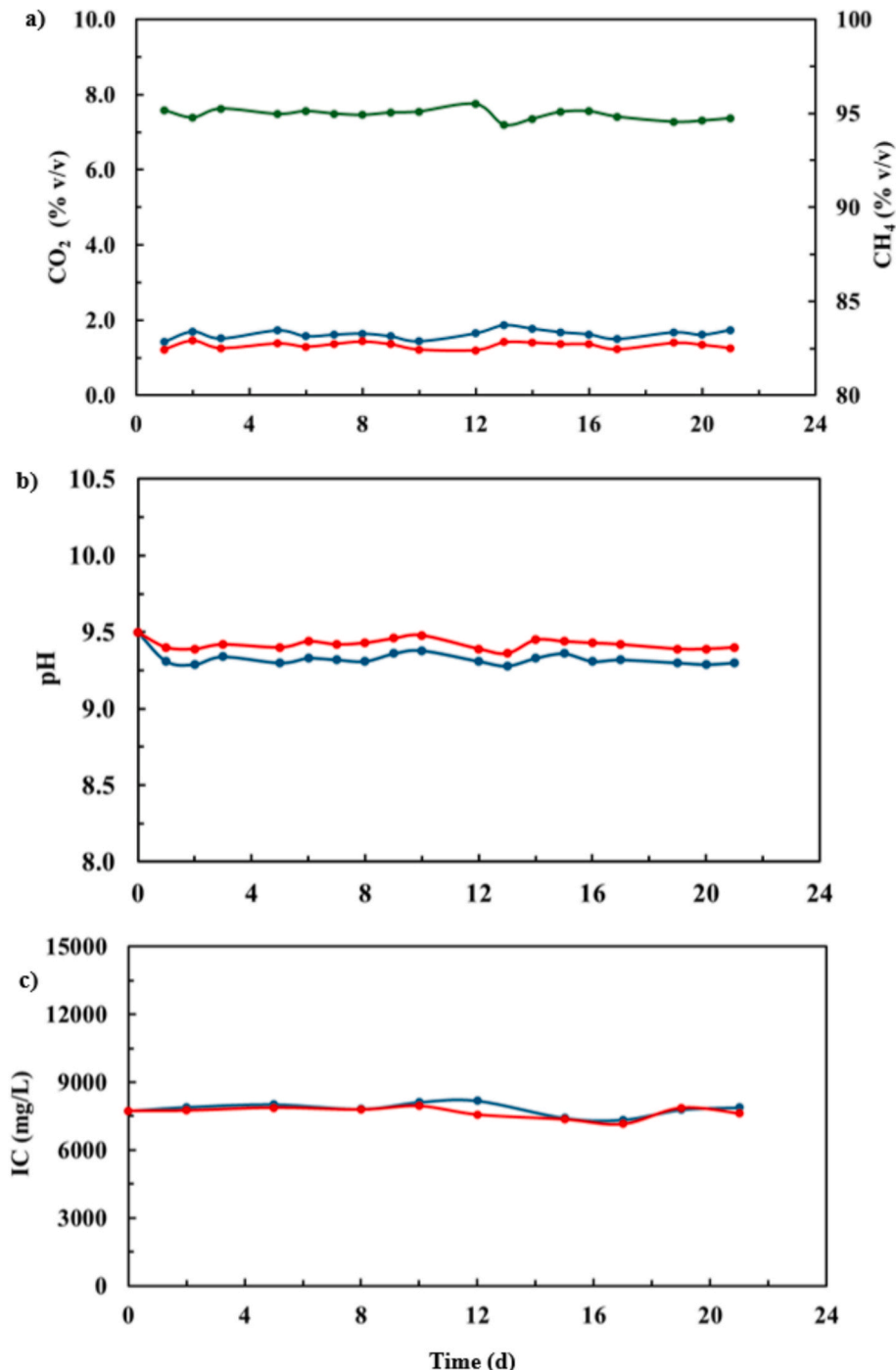


**Fig. 3.** Time course of a) biomethane  $\text{CO}_2$  concentration (blue line),  $\text{CO}_2$  concentration in the outlet air (red line) and biomethane  $\text{CH}_4$  concentration (green line); b) pH in the absorption column (blue line) and pH in the desorption column (red line); and c) IC in the absorption column (blue line) and IC in the desorption column (red line). Optimal operating conditions: BF = 90 L/d, AF = 1500 L/d, IC = 8000 mg/L, initial pH = 9.5, L/G = 0.7 and Fe = 5 Mm. (For interpretation of the references to colour in this figure legend, the reader is referred to the web version of this article.)

strategy to mitigate methane loss may be to use another solvent that requires less air flow for regeneration, or that solubilizes lower CH<sub>4</sub> concentrations in the absorption column. The steady-state pH in the absorption and desorption columns accounted for 9.3 ± 0.0 and 9.4 ± 0.0, respectively, while the steady-state IC in the absorption and desorption columns was 8900 ± 370 and 8650 ± 410 mg/L, respectively. H<sub>2</sub>S was completely dissolved and then chemically oxidized with dissolved oxygen, as it was not detected in either the biomethane or the exhaust air. Dissolved H<sub>2</sub>S is in chemical equilibrium with HS<sup>-</sup> and S<sup>2-</sup> ions depending on the pH. At pH = 9–11, the HS<sup>-</sup> ion is the dominant species with a ~100 % share [25]. During the three weeks of experiment, the concentration of HS<sup>-</sup> averaged 5 ± 2 mg S/L, which was negligible considering the concentration that would be reached if all the H<sub>2</sub>S absorbed from the biogas were dissolved in the aqueous medium (~1110 mg S/L). It can be hypothesized that the H<sub>2</sub>S absorbed was continuously oxidized with dissolved O<sub>2</sub>. According to Millero (1986) [26], HS<sup>-</sup> can be oxidized to polysulfides (S<sub>4</sub><sup>2-</sup>, S<sub>5</sub><sup>2-</sup> and S<sub>6</sub><sup>2-</sup>) and thiosulphate when the pH is above 9 (Eq. 1–4). In this sense, the concentrations of S-S<sub>2</sub>O<sub>3</sub><sup>2-</sup> and S-SO<sub>4</sub><sup>2-</sup> in the recirculating medium were measured at the end of the experiment, resulting in 508 ± 18 mg S/L and 6 ± 1 mg S/L, respectively. This entails that the main mechanisms of sulphur removal from biogas were the partial oxidation of H<sub>2</sub>S to thiosulphate (~500 mg S/L) and likely polysulfides (~600 mg S/L).

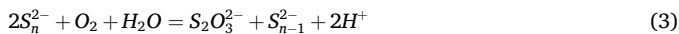
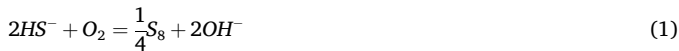


Fig. 3 shows the time course of biomethane composition, pH and IC during three weeks of operation under the optimal operational conditions above described with an EDTA-Fe concentration of 5 mM. The biomethane composition averaged 1.7 ± 0.1 % CO<sub>2</sub>, 0.7 ± 0.1 % O<sub>2</sub>, 2.7 ± 0.3 % N<sub>2</sub> and 94.9 ± 0.4 % v/v CH<sub>4</sub>. The outlet air composition averaged 1.4 ± 0.1 % CO<sub>2</sub>, 20.0 ± 0.1 % O<sub>2</sub>, 78.3 ± 0.1 % N<sub>2</sub> and 0.3 ± 0.1 % v/v CH<sub>4</sub>, which resulted in a CO<sub>2</sub> removal efficiency of 97 % and a CH<sub>4</sub> slip of 6 %. The pH in the absorption and desorption columns under steady-state conditions accounted for 9.3 ± 0.0 and 9.4 ± 0.0, respectively, while the IC in the absorption and desorption columns was 7820 ± 270 and 7670 ± 247 mg C/L, respectively. The average concentration of HS<sup>-</sup> in the solvent was negligible (2 ± 1 mg S/L), while the concentrations of thiosulphate and sulphate at the end of the experiment accounted for 30 ± 8 mg S/L and 25 ± 1 mg S/L, respectively. In this context, most of the H<sub>2</sub>S removed from the biogas was oxidized to elemental sulphur by reducing EDTA-Fe<sup>3+</sup> to EDTA-Fe<sup>2+</sup> [18,27].

### 3.5. Energy analysis

The energy consumption of this low cost technology per Nm<sup>3</sup> of biogas treated under optimal conditions was estimated according to Marín et al. (2020) [3] (Eq. (5) and (6)):

$$P_{\text{gas}} = \frac{Q_{\text{gas}} \cdot \Delta P}{0.7} \quad (5)$$

$$P_{\text{liq}} = \frac{Q_{\text{liq}} \cdot \rho \cdot g \cdot H}{0.7} \quad (6)$$

where Q<sub>gas</sub> refers to either the biogas or air flowrate (Q<sub>biogas</sub> = 1.0 × 10<sup>-6</sup> m<sup>3</sup> s<sup>-1</sup>; Q<sub>air</sub> = 1.7 × 10<sup>-5</sup> m<sup>3</sup> s<sup>-1</sup>), ΔP is the pressure drop (200 kPa), Q<sub>liq</sub> is the recirculating solvent flowrate between both columns (7.3 × 10<sup>-7</sup> m<sup>3</sup> s<sup>-1</sup>), g is the gravity constant (9.8 m s<sup>-2</sup>), ρ is the water density (1000 kg m<sup>-3</sup>) and H is the height of liquid in the column (2 m).

The power demand of the system accounted for 5.3 × 10<sup>-3</sup> kW (P<sub>biogas</sub> = 3 × 10<sup>-4</sup> kW + P<sub>air</sub> = 5 × 10<sup>-3</sup> kW + P<sub>liq</sub> = 2 × 10<sup>-5</sup> kW). In this context, the scalability law can be applied to estimate the electricity demand of the process at industrial scale, (Eq. (7)):

$$P_2 = P_1 \cdot \left(\frac{Q_2}{Q_1}\right)^n \quad (7)$$

where P<sub>1</sub> and P<sub>2</sub> are the required powers at the two scales, Q<sub>1</sub> and Q<sub>2</sub> the treated biogas flow rates, and n the scale factor. A typical scale factor for chemical industrial processes of 0.7 was considered. In this context, a P<sub>2</sub> of 14.3 kW can be estimated for an industrial biogas stream Q<sub>2</sub> of 300 Nm<sup>3</sup>/h. Therefore, the electricity requirement of the absorption-stripping process based on EDTA-Fe/carbonate solutions at ambient pressure and temperature accounts for 0.05 kW·h per Nm<sup>3</sup> of biogas treated when applied at industrial scale. This electricity demand is much lower compared to conventional technologies such as water/chemical/organic scrubbing, pressure swing adsorption or membrane separation, which entail an electricity demand of 0.13–0.4 kW·h/Nm<sup>3</sup> of cleaned biogas and thermal demands of 0.4–0.55 kW·h/Nm<sup>3</sup> of cleaned biogas for solvent regeneration [28]. No thermal energy is required in this technology for solvent regeneration, which is carried out via air stripping.

### 3.6. Economic analysis

The scalability law (Eq. (7)) was applied to estimate the volume of the absorption and desorption columns to treat a biogas stream of 300 Nm<sup>3</sup>/h. Considering n = 0.7, the volume of the columns was 20 m<sup>3</sup>. On the other hand, a volume of 3 m<sup>3</sup> was considered reasonable for the degassing chamber. The cost estimate of the equipment was calculated according to [29] (Eq. (8)):

$$Ce = C \cdot S^m \quad (8)$$

where Ce = purchased equipment cost (€), S = characteristic size parameter (m<sup>3</sup> for tanks and kW for compressors/pumps), C = cost constant (€) and m = index for that type of equipment. C and m were obtained from [29] resulting in C = 2800 and 2230, m = 0.6 and 0.8 for tanks and compressors/pumps, respectively. The Chemical Engineering Plant Cost Index (CEPCI) was used to consider the inflation. The result of CEPCI (2022)/CEPCI (2004) = 813/445 was 1.8, hence the cost of the equipment was increased by 80 % to estimate its current value. The cost of the equipment was: columns = 30000 € (per unit), degassing chamber = 10000 €, biogas compressor = 5500 € (it was increased by 60 % because it must be of the ATEX type), air compressor = 32000 € and liquid pump = 2300 €. The total cost of the equipment amounted to 109,800 €. According to the Lang method, the total cost of the plant is the Lang factor (4.1 for solids and fluids processing) multiplied by the cost of the equipment. Therefore, the total cost of the plant amounted to 4.1 × 109800 € ~ 450,000 €.

According to [30], the specific investment cost in conventional technologies for biogas upgrading is 4000 €/(Nm<sup>3</sup>/h) for 300 Nm<sup>3</sup>/h, and the specific electricity demand of 0.20–0.25 kWh/Nm<sup>3</sup>. This means that the investment cost and energy demand of this innovative technology is 2.6 and 4–5 times lower than that of conventional technologies, respectively, which demonstrates its economic potential.

### 4. Conclusions

An innovative and low-cost physicochemical process to simultaneously remove CO<sub>2</sub> and H<sub>2</sub>S from biogas was validated at pilot scale. The absorption-stripping process based on a EDTA-Fe/carbonate solvent and fine bubble membrane diffusers operated at ambient pressure and temperatures supported, under optimal conditions (biogas flowrate of 90 L/d, air flowrate of 1500 L/d, IC of 8000 mg/L, L/G of 0.7 and Fe of 0 mM), the production of a biomethane according to most international

regulations for injection into natural gas grids ( $\text{CH}_4 \geq 90\%$ ,  $\text{CO}_2 \leq 2\%$ ,  $\text{O}_2 \leq 1\%$  v/v and insignificant amounts of  $\text{H}_2\text{S}$ ). The stability of the system was also confirmed by continuous three-week operation experiments. On the other hand, the presence of carbon coated iron based nanoparticles at 300 and 3000 mg L<sup>-1</sup> did not enhance the  $\text{CO}_2$  absorption performance. Interestingly, the environmental and operational conditions implemented in the system allowed for a complete elimination of  $\text{H}_2\text{S}$  via oxidation with the dissolved  $\text{O}_2$  into thiosulphate and likely polysulfides, without the need of additional oxidizing agents such as EDTA-Fe. A preliminary energy analysis demonstrated the greater sustainability of this innovative technology compared to conventional physicochemical processes for biogas upgrading. However, further work should focus on reducing the  $\text{CH}_4$  slip of the process. The economic evaluation of this novel technology demonstrated its economic potential compared to conventional technologies, which currently dominate the biogas upgrading market. Ultimately, this work undoubtedly serves as a foundation for its development on a more commercial scale.

### CRedit authorship contribution statement

**Edwin G. Hoyos:** Writing – original draft, Visualization, Validation, Methodology, Investigation, Formal analysis, Conceptualization. **Saeed Rasekh:** Conceptualization. **Rogelio Mazaeda:** Project administration. **Raúl Muñoz:** Writing – review & editing, Validation, Supervision, Project administration, Funding acquisition, Conceptualization.

### Declaration of competing interest

The authors declare that they have no known competing financial interests or personal relationships that could have appeared to influence the work reported in this paper.

### Acknowledgements

This research was funded by the Spanish Research Agency via the Public-Private Collaboration Programme (CPP2021-008427).

### Appendix A. Supplementary data

Supplementary data to this article can be found online at <https://doi.org/10.1016/j.fuel.2025.138010>.

### Data availability

The data that has been used is confidential.

### References

- Aryal N, Zhang Y, Bajracharya S, Pant D, Chen X. Microbial electrochemical approaches of carbon dioxide utilization for biogas upgrading. *Chemosphere* 2022; 291(P1):132843. <https://doi.org/10.1016/j.chemosphere.2021.132843>.
- Di Profio P, et al. Emerging green strategies for biogas upgrading through  $\text{CO}_2$  capture: from unconventional organic solvents to clathrate and semi-clathrate hydrates. *J Mol Liq* 2023;391(PA):123196. <https://doi.org/10.1016/j.molliq.2023.123196>.
- Marín D, Vega M, Lebrero R, Muñoz R. Optimization of a chemical scrubbing process based on a Fe-EDTA-carbonate based solvent for the simultaneous removal of  $\text{CO}_2$  and  $\text{H}_2\text{S}$  from biogas. *J Water Process Eng* 2020;37:101476. <https://doi.org/10.1016/j.jwpe.2020.101476>.
- Ahmed SF, et al. Biogas upgrading, economy and utilization: a review. *Environ Chem Lett* 2021;19(6):4137–64. <https://doi.org/10.1007/s10311-021-01292-x>.
- Francisco A, Lago T, Abdolmaleki SF, Galera M, Bello Bugallo PM. From biogas to biomethane: an in-depth review of upgrading technologies that enhance sustainability and reduce greenhouse gas emissions. *Appl Sci* 2024;14(6):2342. <https://doi.org/10.3390/app14062342>.
- Schiavon Maia DC, et al. Removal of  $\text{H}_2\text{S}$  and  $\text{CO}_2$  from biogas in bench scale and the pilot scale using a regenerable Fe-EDTA solution. *Renew Energy* 2017;109: 188–94. <https://doi.org/10.1016/j.renene.2017.03.023>.
- Jaiswar G, Dabas N, Chaudhary S, Jain VP. Progress in absorption of environmental carbon dioxide using nanoparticles and membrane technology. *Int J Environ Sci Technol* 2023;20(9):10385–404. <https://doi.org/10.1007/s13762-022-04526-9>.
- Lee JS, Lee JW, Kan TY.  $\text{CO}_2$  absorption/regeneration enhancement in DI water with suspended nanoparticles for energy conversion application. *Appl Energy* 2015;143:119–29. <https://doi.org/10.1016/j.apenergy.2015.01.020>.
- Jeon HS, Park SE, Ahn B, Kim YK. Enhancement of biodiesel production in *Chlorella vulgaris* cultivation using silica nanoparticles. *Biotechnol Bioprocess Eng* 2017;22(2):136–41. <https://doi.org/10.1007/s12257-016-0657-8>.
- Vargas-Estrada L, Hoyos EG, Méndez L, Sebastian PJ, Muñoz R. Boosting photosynthetic biogas upgrading via carbon-coated zero-valent iron nanoparticle addition: a pilot proof of concept study. *Sustain Chem Pharm* 2023;31:100952. <https://doi.org/10.1016/j.scp.2022.100952>.
- Hoyos EG, Amo-duodu G, Kiral UG, Vargas-estrada L, Lebrero R, Muñoz R. Influence of carbon-coated zero-valent iron-based nanoparticle concentration on continuous photosynthetic biogas upgrading. *Fuel* 2024;356:129610. <https://doi.org/10.1016/j.fuel.2023.129610>.
- European Committee for Standardization, “UNE EN 16723-1:2017 Natural Gas and Biomethane for Use in Transport and Biomethane for Injection in the Natural Gas Network - Part 1: Specifications for Biomethane for Injection in the Natural Gas Network,” 2017. <https://www.en-standard.eu/une-en-16723-1-2017-natural-gas-and-biomethane-for-use-in-transport-andbiomethane-%0Afor-injection-in-the-natural-gas-network-part-1-specifications-forbiomethane-%0Afor-injection-in-the-natural-gas-network/>.
- European Committee for Standardization, “UNE EN 16723-2:2018 Natural Gas and Biomethane for Use in Transport and Biomethane for Injection in the Natural Gas Network - Part 2: Automotive Fuels Specification,” 2018. <https://www.en-standard.eu/une-en-16723-2-2018-natural-gas-andbiomethane-%0Afor-use-in-transport-andbiomethane-for-injection-in-the-natural-gasnetwork-%0Apart-2-automotive-fuels-specification/>.
- Roy RK. *Design of experiments using the Taguchi approach: 16 steps to product and process improvement*. New York: Wiley; 2001.
- Alcántara C, García-encina PA, Muñoz R. Evaluation of mass and energy balances in the integrated microalgae growth-anaerobic digestion process. *Chem Eng J* 2013;221:238–46. <https://doi.org/10.1016/j.cej.2013.01.100>.
- Toledo-cervantes A, Serejo ML, Blanco S, Pérez R, Lebrero R, Muñoz R. Photosynthetic biogas upgrading to bio-methane: boosting nutrient recovery via biomass productivity control. *Algal Res* 2016;17:46–52. <https://doi.org/10.1016/j.algal.2016.04.017>.
- Posadas E, Marín D, Blanco S, Lebrero R, Muñoz R. Simultaneous biogas upgrading and centrate treatment in an outdoors pilot scale high rate algal pond. *Bioresour Technol* 2017;232:133–41. <https://doi.org/10.1016/j.biortech.2017.01.071>.
- Frare LM, Vieira MGA, Silva MGC, Pereira NC, Gimenes ML. Hydrogen sulfide removal from biogas using Fe/EDTA solution: gas/liquid contacting and sulfur formation. *Environ Prog Sustain Energy* 2010;29(1):34–41. <https://doi.org/10.1002/ep.10374>.
- Li H.  $\text{CO}_2$  capture by various nanoparticles: recent development and prospective. *J Clean Prod* 2023;414:137679. <https://doi.org/10.1016/j.jclepro.2023.137679>.
- Lee JW, Kim S, Torres Pineda I, Kang YT. Review of nanoabsorbents for capture enhancement of  $\text{CO}_2$  and its industrial applications with design criteria. *Renew Sustain Energy Rev* 2021;138:110524. <https://doi.org/10.1016/j.rser.2020.110524>.
- Taheri M, Mohebbi A, Hashemipour H, Morad A. Simultaneous absorption of carbon dioxide ( $\text{CO}_2$ ) and hydrogen sulfide ( $\text{H}_2\text{S}$ ) from  $\text{CO}_2\text{-H}_2\text{S}\text{-CH}_4$  gas mixture using amine-based nanofluids in a wetted wall column. *J Nat Gas Sci Eng* 2016;28: 410–7. <https://doi.org/10.1016/j.jngse.2015.12.014>.
- Lee JH, Lee JW, Kang YT.  $\text{CO}_2$  regeneration performance enhancement by nanoabsorbents for energy conversion application. *Appl Therm Eng* 2016;103: 980–8. <https://doi.org/10.1016/j.applthermaleng.2016.04.160>.
- Ashrafmansouri SS, Nasr Esfahany M. The influence of silica nanoparticles on hydrodynamics and mass transfer in spray liquid-liquid extraction column. *Sep Purif Technol* 2015;151:74–81. <https://doi.org/10.1016/j.seppur.2015.07.031>.
- Zhang F, Wang X, Wang Q, Yang C, Qiu T. Effect of nanoparticles on interfacial mass transfer characteristics and mechanisms in liquid-liquid extraction by molecular dynamics simulation. *Int J Heat Mass Transf* 2021;173:121236. <https://doi.org/10.1016/j.ijheatmasstransfer.2021.121236>.
- Miloshova M, Baltes D, Bychkov E. New chalcogenide glass chemical sensors for  $\text{S}_2^-$  and dissolved  $\text{H}_2\text{S}$  monitoring. *Water Sci Technol* 2003;47(2):135–40. <https://doi.org/10.2166/wst.2003.0104>.
- Miller FJ. The thermodynamics and kinetics of the hydrogen sulfide system in natural waters\*. *Mar Chem* 1986;18(2–4):121–47. [https://doi.org/10.1016/0304-4203\(86\)90003-4](https://doi.org/10.1016/0304-4203(86)90003-4).
- Schiavon DC, Cardoso FH, Frare LM, Gimenes ML, Pereira NC. Purification of biogas for energy use. *Chem Eng Trans* 2014;37(1):643–8. <https://doi.org/10.3303/CET1437108>.
- Thiruselvi D, et al. A critical review on global trends in biogas scenario with its upgradation techniques for fuel cell and future perspectives. *Int J Hydrogen Energy* 2021;46(31):16734–50. <https://doi.org/10.1016/j.ijhydene.2020.10.023>.
- Sinnott RK. Costing and project evaluation, in *Coulson and Richardson's chemical engineering volume 6 - chemical engineering design*, Fourth., Elsevier, 2005, pp. 243–283.
- Bauer F, Persson T, Hulteberg C, Tamm D. Biogas upgrading - technology overview, comparison and perspectives for the future. *Biofuels Bioprod Biorefining* 2013;7 (5):499–511. <https://doi.org/10.1002/bbb.1423>.